Kinetic Study of the Electrochemical Oxidation of Salicylic Acid and Salicylaldehyde Using UV/vis Spectroscopy and Multivariate Calibration

Nelson Matyasovszky, Min Tian, and Aicheng Chen*

Department of Chemistry, Lakehead University, 955 Oliver Road, Thunder Bay, Ontario P7B 5E1, Canada

Received: May 17, 2009

The electrochemical oxidation of salicylic acid (SA), salicylaldehyde (SH), and their mixtures at Ti/$IrO_2-SnO_2-Sb_2O_5$ electrodes was studied using in situ UV/vis spectroscopy. Plackett-Burman's experimental design was employed to simultaneously investigate the effect of current density, temperature, mass transfer, composition of the electrode materials, initial concentration, and supporting electrolyte on the electrochemical oxidation of SA, revealing that temperature and the applied current density are the two major factors. The kinetics of the electrochemical oxidation of SA and SH was thus investigated at different temperatures and current densities, showing that the electrochemical oxidation of SA and SH is governed by the hydroxyl radical reaction and follows first-order kinetics with the apparent activation energy of 24.8 and 17.2 kJ/mol, respectively. The competitive effects of SA and SH during the electrochemical oxidation of their mixtures were further studied using UV/vis spectroscopy and multivariate calibration.

1. Introduction

Salicylic acid (SA) and salicylaldehyde (SH) are two common organic pollutants that build up in the environment due to the inefficiency of traditional water purification processes.[1] These pollutants find their way into the water system through pharmaceutical medications, cosmetic products, and agricultural chemicals.[2−4] Thus there is an ever increasing growing accumulation of SA and SH in wastewater. The U.S. EPA has recently shown particular concern in compounds that are closely related to salicylic acid.[5,6] As seen in Scheme 1, SA and SH are similar in molecular structure with SA containing an extra hydroxyl group allowing for extensive hydrogen bonding.[7] A variety of techniques including electrochemical oxidation,[8−10] activated electrosorption,[11] chemical and photochemical oxidation,[12−17] and biological digestion[18] have been used to treat polluted water. Although the biological process is currently the most economical process for wastewater treatment, its application is not always possible, especially for effluents with high concentrations of organic or toxic compounds. Previous studies have shown that advanced oxidation processes (AOPs) such as photochemical and electrochemical methods provide environmentally friendly removal of many organic pollutants.[8−10,12−17] The advanced oxidation processes involve the generation of hydroxyl radicals to oxidize harmful pollutants;[19−22] the ability of the advanced oxidation processes to eliminate pollutants can be credited to the strong oxidation power of the hydroxyl radial (E°, 2.80 vs SHE).[1,21,22]

Electrochemical oxidation is an advanced oxidation process where electrons are used primarily to fuel the reaction.[23] The electrochemical oxidation process allows easy operation under a wide range of conditions and can produce desired products while still continuing to be environmentally friendly.[9,24] The efficiency and performance of the electrochemical oxidation process is highly dependent on the electrode's composition.[23,25] The electrochemical treatment of contaminated water with tin- and antimony-based electrodes (Ti/$SnO_2-Sb_2O_5$) has shown promising results, based on their "high-over potential for oxygen evolution" and their ability to produce hydroxyl radicals (•OH).[9] The low costs make the tin- and antimony-based electrodes promising for commercial application; however, they experience a very short service life.[9] Previous studies have revealed that the addition of iridium to the tin and antimony electrodes can greatly extend service life without large detrimental impacts on performance.[26,27]

SCHEME 1: Chemical Structure of Salicylic Acid and Salicylaldehyde

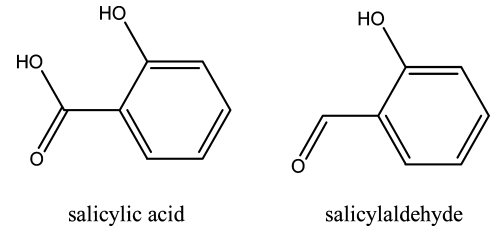

In this study, for the first time, we report on the electrochemical oxidation of salicylic acid and salicylaldehyde as the model organic pollutants at Ti/$IrO_2-SnO_2-Sb_2O_5$ electrodes. Plackett-Burman experimental design is utilized to identify the factors (e.g., mass transfer, concentration, current, electrolyte, temperature, and electrode composition) that may have a major impact on the oxidation process. In addition, more than one organic compound is frequently present in wastewater; thus competitive effects are expected in wastewater treatment and must be considered. UV spectroscopy and multivariate calibration are employed to evaluate competitive effects during the electrochemical oxidation of mixtures of SA and SH.

2. Experimental Section

2.1. Materials. Salicylic acid (99+%) and salicylaldhyde (98%) of reagent grade were purchased from Sigma-Aldrich and used without any further purification. All other chemicals used are reagent grade unless otherwise stated. The water (18.2 MΩcm) used for all experimental solutions was purified by a Nanopure water system.

* To whom correspondence should be addressed. Tel.: +1 807 343 8318. Fax: +1 807 346 7775. E-mail address: aicheng.chen@lakeheadu.ca.

10.1021/jp904602j CCC: $40.75
Published on Web 07/30/2009

2.2. Preparation and Characterization of the Electrodes. The $Ti/IrO_2-SnO_2-Sb_2O_5$ electrodes used in this study were prepared using a thermal decomposition method.[28,29] Titanium strips were sonicated in acetone for 10 min and in pure water for another 10 min to degrease the surfaces. The strips were etched in 18% hydrochloric acid at 85 °C for 15 min. To prepare the coating solutions, 0.90 g of $IrCl_3 \cdot 3H_2O$ was dissolved in 10.27 g of ethanol; 2.31 mL of antimony-doped polymeric precursor of tin oxide from Alfa Aesar was dissolved in 23.1 mL of isopropanol. To ensure that the solutes had dissolved into the solution, the mixtures were placed in a Cole-Parmer sonicator for a period of 20 min. The coating solutions were made by mixing the previously mentioned solutions together to achieve different percentages of iridium in the coating. The Ti strips were painted with the coating solution and the solvents were evaporated in an air stream at 80 °C. After each coat, the strips were baked for a period of 10 min at 450 °C. This painting process was repeated until the substrates had a coating load of 30.0 g/m^2. A final bake was carried out at 450 °C for a period of 1 h to ensure that the thermal oxidation process was complete. The morphology of the electrocatalytic coatings was examined using a JEOL 5900LV scanning electron microscopy and X-ray energy dispersive spectrometry (SEM/EDX).

2.3. Optical Absorbance Measurements. A Cary 50 type UV−vis spectrophotometer was used to measure the absorbance of the electrochemical oxidation of SA and SH. In order to determine the concentration, the absorbance readings were converted to concentrations using the absorbance−concentration calibrations for both SH and SA. Salicylaldehyde's relationship was $C = 8.63 \times 10^{-2}A + 1.56 \times 10^{-3}$ at the 256 nm peak, while salicylic acid's relationship was $C = 2.83 \times 10^{-2}A + 5.88 \times 10^{-2}$ at the 236 nm peak.

2.4. Electrochemical Cell. An Arbin Instruments power supply coupled with a computer system was used to constantly monitor the current and potential. A platinum coil was used as the counter electrode and a 1.0 cm^2 $Ti/IrO_2-SnO_2-Sb_2O_5$ was used as the working electrode. A Fisher water bath was used for temperature control and a Fisher stirrer was used to stir the solution during the electrochemical oxidation of the salicylic acid and salicylaldehyde.

3. Results and Discussion

3.1. Characterization of the Fabricated $Ti/SnO_2-Sb_2O_5-IrO_2$ Electrodes. The morphology of the prepared $Ti/IrO_2-SnO_2-Sb_2O_5$ electrodes was characterized using a JEOL 5900LV SEM/EDX. Figure 1A shows the SEM images of $IrO_2-SnO_2-SbO_5$ electrodes prepared through the thermal decomposition method. It can be seen that the film exhibits a typical porous "crack mud" structure with average width ca. 2 μm, which is different from the compact and nonporous polycrystalline structure of the film prepared with the "spray pyrolysis technique".[30] Figure 1B is the EDS spectrum of the $IrO_2-SnO_2-SbO_5$, displaying peaks for oxygen, iridium, tin, and antimony. Further quantitative analysis revealed that the coating contained about 10% IrO_2, which is consistent with the prepared precursor solutions used in the fabrication process.

3.2. Electrochemical Oxidation of Salicylaldehyde and Salicylic Acid. The electrochemical oxidation of SA and SH was conducted at the $Ti/IrO_2-SnO_2-Sb_2O_5$ electrode. Figure 2A shows typical scanning kinetics during the electrochemical oxidation of 30 ppm salicylic acid at 40 °C and 100 mA. The UV−vis spectra were taken every 5 min for the first 20 min and then every 10 min for the remaining 70 min. As shown in Figure 2A, there are two absorbance peaks with maxima at 236 and 302 nm, respectively. The intensity of the two peaks

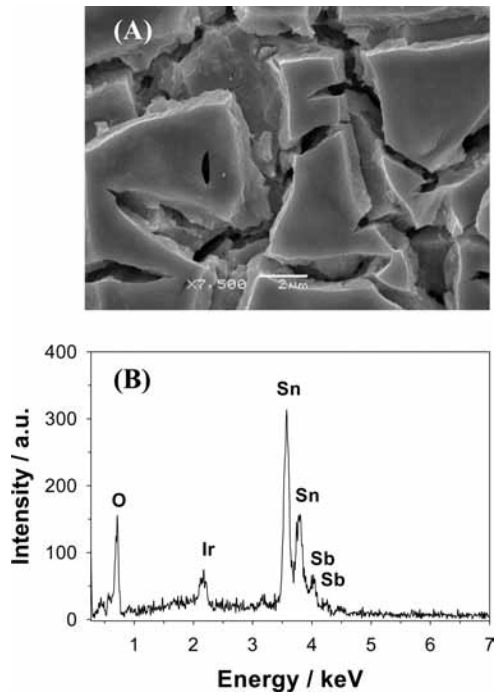

Figure 1. SEM images (A) and EDS (B) of the as-prepared $Ti/IrO_2-SnO_2-Sb_2O_5$.

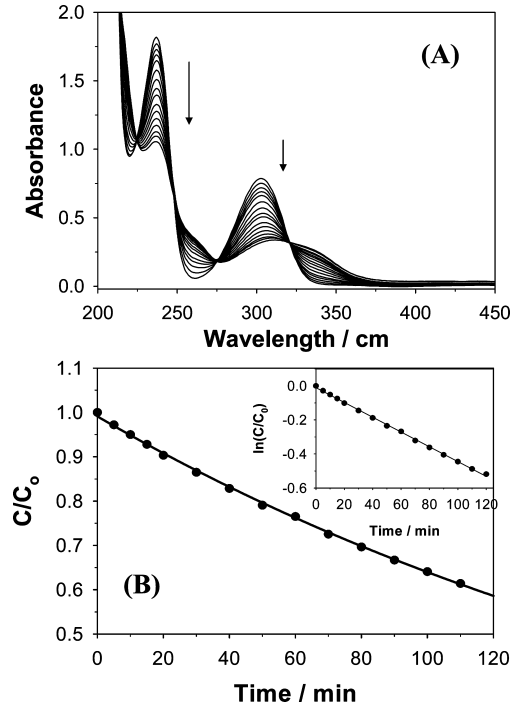

Figure 2. (A) The absorbance spectra for the electrochemical oxidation of 30 ppm salicylic acid at a $Ti/IrO_2-SnO_2Sb_2O_5$ electrode in 0.5 M H_2SO_4 at 40 °C with 100 mA. (B) The corresponding C/C_o vs time ($c/c_o - t$) curves for the simulation data based on first-order kinetics (solid line) and the experimental results (solid circles). The inset shows $\ln(C/C_o) - t$ relationship.

decreases with respect to the electrochemical oxidation time, indicating that the salicylic acid was being oxidized. The concentration−time relationship was calculated based on the calibration equation between the absorbance versus concentration presented in Section 2.3. As shown in Figure 2B, after the 120 min period of treatment 40% of the initial salicylic acid was oxidized. The regression curve based on first-order kinetics fits very well with the experimental data. The $\ln(C/C_o) - t$

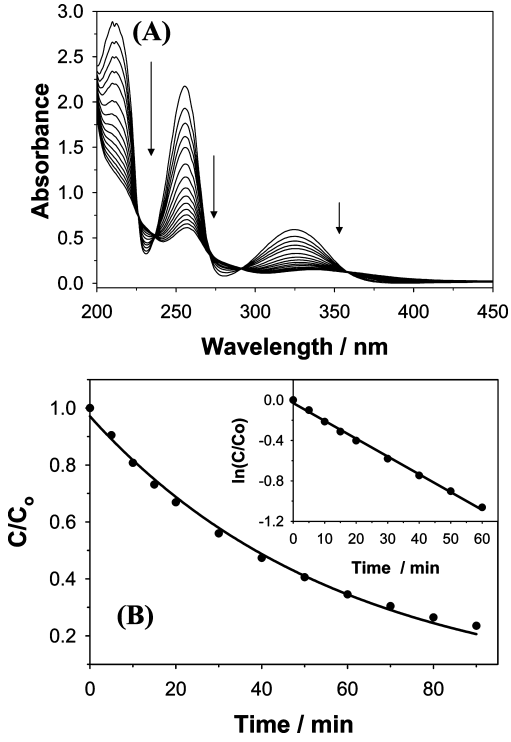

Figure 3. (A) The absorbance spectra for the electrochemical oxidation of 30 ppm salicylaldehyde at a Ti/IrO_2−SnO_2−Sb_2O_5 electrode in 0.5 M H_2SO_4 at 40 °C with a 100 mA. (B) The corresponding C/C_o vs time ($c/c_o - t$) curves for the simulation data based on first-order kinetics (solid line) and the experimental results (solid circles). The inset shows $\ln(C/C_o) - t$ relationship.

relationship shown in the inset of Figure 2B further supports the first-order kinetics relationship with a correlation coefficient of 0.999. The first-order kinetics electrochemical oxidation process was determined to have a rate constant of $k = 4.34 \times 10^{-3}\text{min}^{-1}$.

Figure 3A presents the absorbance spectra for the electrochemical oxidation of SH with readings taken every 5 min during the first 20 min and then every 10 min for the remaining 70 min. The absorbance spectra display three peaks centered at 211, 256, and 325 nm; their intensity decreases with respect to time. The calibration curve for salicylaldehyde (Section 2.3) was used to transform the measured absorbance into concentration. As seen in Figure 3B, the concentration of the salicylaldehyde remaining after 90 min of electrochemical treatment was only 23.5% of the initial concentration. The regression curve in Figure 3B shows the relationship between the experimental data and first-order kinetics for the $C/C_o - t$ relationship. The first-order kinetics correlation was determined to have a rate constant of $k = 1.72 \times 10^{-2}$ min^{-1} and was further supported through a 0.997 correlation coefficient for the linear relationship of the $\ln(C/C_o) - t$ (inset). It is interesting to note that the rate constant for the electrochemical oxidation of SH is ca. 4 times larger than that for the electrochemical oxidation of SA. It has been reported that there are both inter- and intramolecular hydrogen bonds in SA.[7] Two intermolecular hydrogen bonds form cyclic structures typical to carboxylic acid dimers. There is also a strong intramolecular hydrogen bond between the hydroxyl group and the carboxyl group. In contrast, there are only intramolecular hydrogen bonds in SH.

3.3. Plackett-Burman Experimental Design. In the classical experimental approach one variable is held constant while the others are systematically changed "one by one". With this approach the number of experiments is $N_{exp} = L^n$, where L is the number of levels of each variable and n is the number of variables.[31] For instance, an experiment with six different variables testing at three levels (i.e., low, middle, high) would have 729 experiments. To minimize the amount of experiments and decrease the risk of experimental error, Plackett-Burman's experimental design has been used.[32,33] This factorial design can greatly reduce the number of experiments, while still identifying the impact of each variable.[31] Table 1 shows the Plackett-Burman experimental design in this study, consisting of fifteen experiments with six variables testing at three different levels for the electrochemical oxidation of salicylaldehyde. Rate constants are derived from the slope of the $\ln(C/C_o) - t$ curve, which were obtained from the peak centered at 256 nm of the SH absorbance.

The information in Table 1 was used to determine which of the six variables has the largest impact on the rate constant for the electrochemical oxidation process. Using a technique proposed by Rogan et al.,[31] the main effect (ME) of each of the variables was determined using eq 1. The main effect of a variable was calculated and expressed as a percentage of the middle condition. The middle condition was experiment no. 8, where all of the variables were at their middle level

$$\%\text{ME} = \frac{[(x)_1 - (x)_2] \times 100}{(x)_M \times N_{exp}} \quad (1)$$

where $(x)_M$ is the average rate constant at the middle level, N_{exp} is the number of experiments which is totaled fifteen, $(x)_1$ is the mean rate constant at the high parameter, and $(x)_2$ is the mean rate constant at the low parameter.[31]

Using eq 1 and the rate constants from Table 1, the main effect (ME%) of the concentration, electrolyte, electrode composition, current density, mass transfer, and temperature were calculated, as also shown in Table 1. The results show that electrode composition and concentration have minor impacts (e.g., ME 5.9 and 4.3%) on the rate constant, while mass transfer and electrolyte have moderate impacts (e.g., ME 7.9 and 6.4%). It is interesting to note that temperature and current density have the major impacts on the process of oxidation with a main effect of 10.9 and 10.3%, respectively. With the information provided by the Plackett-Burman experimental design, two variables (temperature and current) were further investigated for the electrochemical oxidation of both SH and SA.

3.4. The Influence of Temperature on the Electrochemical Oxidation of Salicylic Acid and Salicylaldehyde. The effect of temperature on the kinetics of the electrochemical oxidation of salicylic acid and salicylaldehyde was studied in the range of 2 to 60 °C at a 100 mA current. The temperature was regulated by a Fisher water bath. Figure 4A shows the $\ln(C/C_o)$ versus time relationship for the electrochemical oxidation of salicylic acid at the different temperatures. The increase in temperature had a positive effect on the electrochemical oxidation of salicylic acid. The rate constant changed with an increase in temperature from 1.45×10^{-3} min^{-1} at 2 °C to 7.29×10^{-3} min^{-1} at 60 °C. Figure 4B shows temperature's effect on the electrochemical oxidation of salicylaldehyde. The $\ln(C/C_o)$ versus time relationship revealed that the rate constant increased from 5.58×10^{-3} to 1.93×10^{-2} min^{-1} with the increase in temperature from 2 to 60 °C, respectively.

Examination of Figure 4A,B reveals that the rate constant for the electrochemical oxidation of salicylic acid experienced less variation accredited to temperature change than the similar salicylaldehyde treatment. It is known that there is extensive

TABLE 1: Plackett-Burman Experimental Design with the Achieved Rate Constant for Salicylaldehyde

expt	current (mA)	temp (°C)	stirring speed	electrodes (%Ir)	conc (ppm)	electrolytes 0.5 M	rate const (min^{-1})
1	20	20	low	5	10	NaOH	1.69×10^{-3}
2	20	2	low	10	5	Na_2SO_4	1.21×10^{-3}
3	20	2	off	10	10	NaOH	5.01×10^{-4}
4	50	2	off	5	10	Na_2SO_4	1.20×10^{-3}
5	20	20	off	5	5	Na_2SO_4	1.43×10^{-3}
6	50	2	low	5	5	NaOH	2.21×10^{-3}
7	50	20	off	10	5	NaOH	2.03×10^{-3}
8	50	20	low	10	10	Na_2SO_4	3.08×10^{-3}
9	50	20	high	10	30	H_2SO_4	3.84×10^{-3}
10	50	40	low	30	30	H_2SO_4	5.05×10^{-3}
11	100	20	high	30	30	Na_2SO_4	3.06×10^{-3}
12	50	40	high	30	10	Na_2SO_4	5.25×10^{-3}
13	100	40	high	10	10	Na_2SO_4	9.57×10^{-3}
14	100	40	low	10	30	H_2SO_4	5.10×10^{-3}
15	100	20	low	30	10	H_2SO_4	6.13×10^{-3}
ME%	10.3	10.9	7.9	5.9	4.3	6.4	

hydrogen bonding between SA, SH, and water.[7] The increase in temperature not only enhances the diffusion of the SA and SH to the electrode surface but also assists in breaking the hydrogen bonding. The Arrhenius relationship for SA and SH estimated from the kinetics data are presented in Figure 5. Salicylic acid's activation energy was 24.8 kJ/mol, which is significantly higher than the 17.2 kJ/mol for electrochemical oxidation of salicylaldehyde. This substantial difference in the activation energies accounts for the profound difference in temperature's influence on the rate constants of SA and SH (Figure 4A,B). These values are quite close to those for hydroxyl radical reactions,[34−36] suggesting that the electrochemical oxidation of SA and SH is governed by radical reaction.

3.5. The Effect of Current Density on the Electrochemical Oxidation of Salicylic Acid and Salicylaldehyde. We further investigated the effect of current density on the electrochemical oxidation of salicylic acid and salicylaldehyde. Various currents were applied, increasing from 50 to 150 mA. UV/vis spectroscopy was used to monitor the time-dependent absorbance of SA and SH during the course of the electrochemical oxidation, and these absorbance readings were converted to concentration using the calibration plots described in Section 2.3. The calculated rate constants obtained from the $\ln(C/C_o) - t$ relationship are shown in Table 2. The rate constant of electrochemical oxidation of salicylic acid varies from 3.51×10^{-3} to 4.89×10^{-3} min^{-1} at 50 and 125 mA, respectively. Salicylic acid's rate constant is positively affected by a current increase in all experimental cases. However, each consecutive enhancement in the rate constant due to an increase in current is smaller than the previous one. Salicylaldehyde also experiences a positive electrochemical oxidation effect from the increase in current density at the selected experimental levels. With an applied current of 125 mA, the rate constant is 0.0189 min^{-1}, which is significantly larger than the 0.0126 min^{-1} experienced at 50 mA. The higher the current density, the more prominent the enhancement of the rate constant for the electrochemical oxidation of salicylaldehyde.

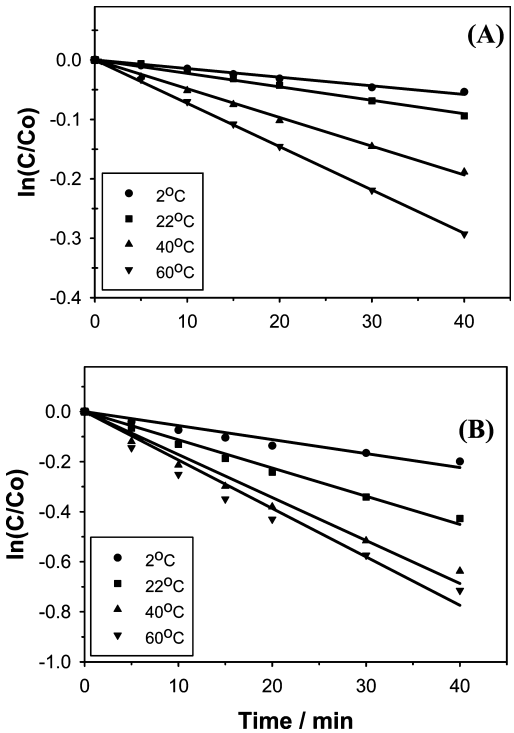

Figure 4. (A) The $\ln(C/C_o) - t$ relationship for temperatures effect on the electrochemical oxidation of 30 ppm (A) SA and (B) SH in 0.5 M H_2SO_4 with 100 mA.

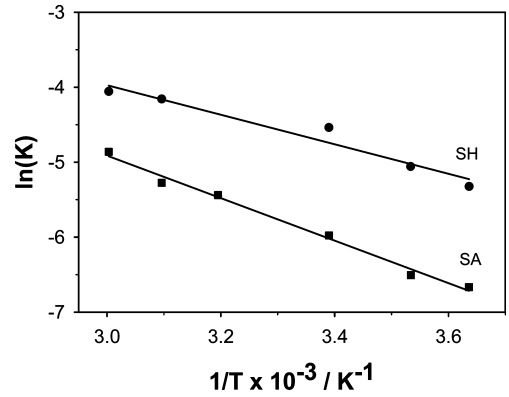

Figure 5. The Arrhenius relationship ($\ln(k) - 1/T$) with a slope utilized in the determination of the activation energy of SA and SH.

TABLE 2: Currents Effect on the Electrochemical Oxidation of 30 ppm SA and SH at 40 °C

	rate constant (min^{-1})	
current (mA)	salicylic acid (SA)	salicylaldehyde (SH)
125	4.89×10^{-3}	1.89×10^{-2}
100	4.65×10^{-3}	1.57×10^{-2}
75	4.21×10^{-3}	1.40×10^{-2}
50	3.51×10^{-3}	1.26×10^{-2}

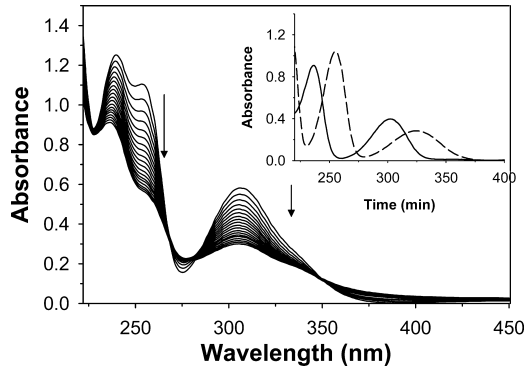

Figure 6. The absorbance spectra for the electrochemical oxidation of SA and SH at a $Ti/IrO_2-SnO_2-Sb_2O_5$ electrode. The applied current was 100 mA, the temperature 40 °C, and the concentration was 15 ppm for each contaminant.

3.6. Electrochemical Oxidation of Mixture of Salicylic Acid and Salicylaldehyde at a $Ti/IrO_2-SnO_2-Sn_2O_5$ Electrode. Figure 6 presents the time dependent spectral absorbance of 15 ppm SA and 15 ppm SH in 0.5 M H_2SO_4 taken at 5 min intervals during the course of electrochemical oxidation at 40 °C. The absorbance of the mixture decreases from 1.02 to 0.57 after 1.5 h of electrolysis at 100 mA. Two isosbestic points at 281 and 348 nm are observed. It can be seen in the inset of Figure 6 that the spectral absorbance of SA and SH overlaps seriously in most regions, thus making it difficult to estimate the concentration using univariate calibrations. One solution to this problem is to apply chemometric analysis techniques. Multivariate calibrations, such as principle component regression and partial least-squares (PLS), differ from traditional, or univariate calibrations, in that an entire spectrum rather than selected peak or peaks is correlated with some known quantity.

Principal component regression (PCR) is considered as a more advanced way of determining the pseudo inverse of the training data needed to predict consistent concentration based on its spectrum. The first step is to obtain a series of spectra (X). These spectra can be collected via several techniques, including UV/vis spectrometry, near-infrared spectrometry, and nuclear magnetic resonance. The next step is to perform principal components analysis[33] on spectra to obtain scores and loadings

$$X = T \cdot P \tag{2}$$

where T and P represent scores and loadings, respectively. The dependent variable is then regressed on these scores to obtain a regression vector, instead of using the measured variables directly.

$$C = T \cdot R \tag{3}$$

Because the principal components (PCs) are factors that capture the greatest amount of variance in the predictor variables, regression is effectively refined to a few important factors in contrast to the MLR approach, which considers all variables. Principal component regression has proven to be relatively less sensitive to spectral noise and other uncorrelated sources of variation than univariate calibrations and is thus generally a more robust predictor.

To obtain the calibration matrix for applying the PCR analysis, 24 solutions of each of the pure components (SA and SH) were prepared with concentrations in the ranges 5−35 and 5−30 ppm, respectively. The objectives of this experiment design are to span the concentration of SA and SH in the calibration set and to obtain the highest level of variability. A crucial decision is to determine how many PCs should be retained. Leave One Out (LOO) cross-validation is commonly used to determine the number of PCs for a good predictive ability. Once the PCR model has been applied to test set and demonstrates the good predictive abilities, it can be used to predict the concentration profiles during the electrochemical oxidation of SA and SH. Table 3 presents the results obtained using PCR. As can be seen, relative errors of less than 5% were found in all test sample sets, showing a high predictive ability of the model. The PCR model was thus employed to predict the concentration profiles of SA and SH during the course of the electrochemical oxidation of the mixtures of SA and SH. The $C/C_o - t$ relationship is displayed in Figure 7A for each SA and SH in the mixture (—) and in a sole solution (----). When comparing the mixture and the separate treatment, the rate constant of the separate oxidation is enhanced. Figure 7B presents the $\ln(C/C_o) - t$ relationship, further confirming the trend found between the mixture and the single component solution. For salicylic acid, the rate constant was 3.26×10^{-3} and 4.50×10^{-3} min^{-1} for the mixture and individual oxidation, respectively. Salicylaldehyde experienced a decrease in the rate constant from 0.0197 min^{-1} in the individual oxidation to 9.08

TABLE 3: The SA and SH Preparation Concentrations Are Depicted against the Calculated Values

SH/ppm			SA/ppm		
actual	predicted	RD%	actual	predicted	RD%
5	5.2	4.6	35	34.6	−1.0
10	9.7	−2.7	30	29.4	−1.9
15	14.6	−3.0	25	24.6	−1.4
20	19.1	−4.3	20	19.7	−1.4
25	25.9	3.5	15	15.2	1.4
30	29.8	−0.5	10	10.1	1.5

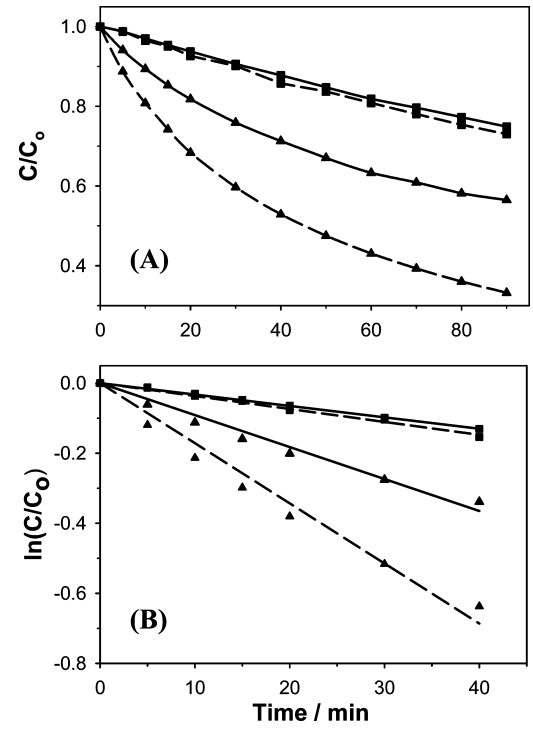

Figure 7. (A) The $C/C_o - t$ and (B) the $\ln(C/C_o) - t$ relationship for the electrochemical oxidation of a 15 ppm mixture of SA (■) and SH (▲) in mixture (—) and in a sole solution (----).

$\times 10^{-3}$ min^{-1} in the mixture. The decrease in a mixture may be accredited to the competition that occurs between SA and SH for catalytic sites.

4. Conclusions

In summary, the kinetics of the electrochemical oxidation of salicylic acid, salicylaldehyde, and their mixtures at Ti/$IrO_2-SnO_2-Sb_2O_5$ electrodes has been studied using in situ UV/vis spectroscopy and multivariate calibration. To the best of our knowledge, for the first time Plackett-Burman design was employed to simultaneously investigate the effect of current density, temperature, mass transfer, composition of the electrode materials, initial concentration, and supporting electrolyte on the electrochemical treatment of pollutants. Our study has shown that temperature and the applied current density are the two major factors, strongly affecting the rate constant of electrochemical oxidation of SA. The activation energy was calculated to be 17.2 and 24.8 kJ/mol for the electrochemical oxidation of SA and SH, respectively. When increasing the current density from 50 to 125 mA/cm^2, the rate constant increased 50% for the electrochemical oxidation of SH and 39% for the electrochemical oxidation of SA. A principal component regression model has been built up for the quantitative study of the electrochemical oxidation of SA and SH mixtures revealing a strong competitive effect. The rate constant for the electrochemical oxidation of SA decreased approximately 27%, from 4.50×10^{-3} min^{-1} in the absence of SH to 3.26×10^{-3} min^{-1} in the mixture; the rate constant for the electrochemical oxidation of SH decreased 54%, from 1.97×10^{-2} min^{-1} in the absence of SA to 9.08×10^{-3} min^{-1} in the SA and SH mixture.

Acknowledgment. This work was supported by a Discovery Grant from the Natural Sciences and Engineering Research Council of Canada (NSERC). A.C. acknowledges NSERC and the Canada Foundation of Innovation (CFI) for the Canada Research Chair Award in Material and Environmental Chemistry.

References and Notes

(1) Adán, C.; Coronado, J. M.; Bellod, R.; Soria, J.; Yamaoka, H. *Appl. Catal., A* **2006**, *303*, 199.
(2) Vilambi, N. R. K.; Chin, D. T. *J. Electrochem. Soc.* **1987**, *134*, 3074.
(3) Mills, A.; Holland, C. E.; Davies, R. H.; Worsley, D. *J. Photochem. Photobiol., A* **1994**, *83*, 257.
(4) Carlotti, M. E.; Sapino, S.; Trotta, M.; Vione, D.; Minero, C.; Peira, E. *J. Disper. Sci. Technol.* **2007**, *28*, 805.
(5) Flaherty, S.; Wark, S.; Street, G.; Farley, J. W.; Brumley, W. C. *Electrophoresis* **2002**, *23*, 2327.
(6) Peremitina, S. P.; Volgina, T. N.; Novikov, V. T. *Russ. J. Applied Chem.* **2008**, *81*, 1081.
(7) Wójcik, M. J. *J. Mol. Struct.* **2005**, *735*, 225.
(8) Quiroz, M. A.; Reyna, S.; Martinez-Huitle, C. A.; Ferro, S.; De Battisti, A. *Appl. Catal., B* **2005**, *59*, 259.
(9) Tian, M.; Bakovic, L.; Chen, A. *Electrochim. Acta* **2007**, *52*, 6517.
(10) Borras, C.; Laredo, T.; Scharifker, B. R. *Electrochim. Acta* **2003**, *48*, 2775.
(11) Ayranci, E.; Conway, B. E. *J. Electroanal. Chem.* **2001**, *513*, 100.
(12) Vinodgopal, K.; Hotchandani, S.; Kamat, P. V. *J. Phys. Chem.* **1993**, *97*, 9040.
(13) Leng, W. H.; Zhu, W. C.; Ni, J.; Zhang, Z.; Zhang, J. Q.; Cao, C. N. *Appl. Catal., A* **2006**, *300*, 24.
(14) Li, J.; Zhang, X.; Ai, Z.; Jia, F.; Zhang, L.; Lin, J. *J. Phys. Chem. C* **2007**, *111*, 6832.
(15) Tian, M.; Wu, G. S.; Adams, B.; Wen, J. L.; Chen, A. *J. Phys. Chem. C* **2008**, *112*, 825.
(16) Yun, H. J.; Lee, H.; Joo, J. B.; Kim, W.; Yi, J. *J. Phys. Chem. C* **2009**, *113*, 3050.
(17) Tian, M.; Adams, B.; Wen, J.; Asmussen, R. M.; Chen, A. *Electrochim. Acta* **2009**, *54*, 3799.
(18) O'Connor, O. A.; Young, L. Y. *Environ. Toxicol. Chem.* **1989**, *8*, 853.
(19) Cañizares, P.; Paz, R.; Sáez, C.; Rodrigo, M. A. *Electrochim. Acta* **2008**, *53*, 2144.
(20) Brillas, E.; Mur, E.; Sauleda, R.; Sánchez, L.; Peral, J.; Domènech, X.; Casado, J. *Appl. Catal., B.* **1998**, *16*, 31.
(21) Zhou, M.; He, J. *Electrochim. Acta* **2007**, *53*, 1902.
(22) Faouzi, M.; Cañizares, P.; Gadri, A.; Lobato, J.; Nasr, B.; Paz, R.; Rodrigo, M. A.; Saez, C. *Electrochim. Acta* **2006**, *52*, 325.
(23) Martinez-Huitle, C. A.; Ferro, S. *Chem. Soc. Rev.* **2006**, *35*, 1324.
(24) Ai, S.; Wang, Q.; Li, H.; Jin, L. *J. Electroanal. Chem.* **2005**, *578*, 223.
(25) Panizza, M.; Cerisola, G. *Electrochim. Acta* **2005**, *51*, 192.
(26) Adams, B.; Tian, M.; Chen, A. *Electrochim. Acta* **2009**, *541*, 491.
(27) Chen, X.; Chen, G. J. *Electrochem. Soc.* **2005**, *152*, J59.
(28) Chen, A.; Nigro, S. *J. Phys. Chem. B* **2003**, *107*, 13341.
(29) Chen, A.; Miller, B. *J. Phys. Chem. B* **2004**, *108*, 2245.
(30) Correa-Lozan, B.; Comninellis, C.; De Battisti, A. *J. Appl. Electrochem.* **1997**, *27*, 970.
(31) Rogan, M. M.; Altria, K. D.; Goodall, D. M. *Chromatographia* **1994**, *38*, 724.
(32) Plackett, R. L.; Burman, J. P. *Biometrika* **1946**, *33*, 33.
(33) Breerton. R. G. *Applied Chemometrics for Scientists*; Wiley: Chichester, England, 2007.
(34) Elliott, A. J.; Simsons, A. S. *Radiat. Phys. Chem.* **1984**, *24*, 229.
(35) Matthews, R. W. *J. Phys. Chem.* **1987**, *91*, 3328.
(36) Chen, D. W.; Ray, A. K. *Water Res.* **1998**, *32*, 3223.

JP904602J